Applied Energy 195 (2017) 659–670

Contents lists available at ScienceDirect

Applied Energy

journal homepage: www.elsevier.com/locate/apenergy

Short-term electrical load forecasting using the Support Vector Regression (SVR) model to calculate the demand response baseline for office buildings

Yongbao Chen [a], Peng Xu [a,*], Yiyi Chu [a], Weilin Li [a], Yuntao Wu [a], Lizhou Ni [b], Yi Bao [b], Kun Wang [b]

[a] School of Mechanical and Energy Engineering, Tongji University, Shanghai 201804, China
[b] Hangzhou Tianli Technology Co., Ltd., Zhejiang 310000, China

HIGHLIGHTS

- A new SVR model to forecast the demand response baseline for office buildings.
- Take temperature two hours before DR event can improve the forecasting accuracy.
- The forecasting accuracy is better than other seven existing methods in DR programs.
- The model is very generic and can be applied to a wide variety of office buildings.

ARTICLE INFO

Article history:
Received 19 August 2016
Received in revised form 7 March 2017
Accepted 9 March 2017
Available online 27 March 2017

Keywords:
Demand respond
SVR model
Short-term baseline
Load forecasting

ABSTRACT

Demand Response (DR) aims at improving the operation efficiency of power plants and grids, and it constitutes an effective means of reducing grid risk during peak periods to ensure the safety of power supplies. One key challenge related to DR is the calculation of load baselines. A fair and accurate baseline serves as useful information for resource planners and system operators who wish to implement DR programs. In the meantime, baseline calculation cannot be too complex, and in most cases, only weather data input is permitted. Inspired by the strong non-linear capabilities of Support Vector Regression (SVR), this paper proposes a new SVR forecasting model with the ambient temperature of two hours before DR event as input variables. We use electricity loads for four typical office buildings as sample data to test the method. After analyzing the model prediction results, we find that the SVR model offers a higher degree of prediction accuracy and stability in short-term load forecasting compared to the other seven traditional forecasting models.

1. Introduction

1.1. Demand response (DR)

Demand Response (DR) is defined as "changes in electric use by demand-side resources from their normal consumption patterns in response to changes in the price of electricity or to incentive payments designed to induce lower electricity use at times of high wholesale market prices or when system reliability is jeopardized" [1]. By moving some energy packages from on-peak periods to valley periods, DR can improve the efficiency of power stations and ensure grid security. At the same time, DR participants can also enjoy benefits such as electricity price decreases and economic subsidies. DR programs are even more important for grids that present high levels of fluctuating generation penetration from renewable energy sources (e.g., photovoltaic power and wind turbines) [2–8].

DR is an important potential demand-side resource for both systems and market operation [9,10], and it has undergone rapid development in the United States and Europe and in the rest of the world. In the United States, due to existing DR resource contributions, the peak load reduction has increased by approximately 10% since 2006 [11]. In Europe, prospects for the future are brighter due to assistance from the European Commission [12]. There are an overall study the regulatory reforms, mark changes and technology development of DR [13]. For China, Beijing, Tangshan, Foshan and Suzhou were selected as DR pilot cities of the National Development and Reform Commission in 2012, meaning that the Chinese government has made DR available to the public. Generally, almost

* Corresponding author.
E-mail address: xupeng@tongji.edu.cn (P. Xu).

http://dx.doi.org/10.1016/j.apenergy.2017.03.034
0306-2619/

Nomenclature

AE	absolute error
BL	baseline
DR	demand response
FUC	fan coil units
ME	mean error
MAE	mean absolute error
PBL	provisional predicted baseline
SVR	support vector regression
VRV	variable refrigerant volume
P	predicted loads, kW
D	electricity loads, kW
M,*N*	days
$\overline{N}$	dataset
$\boldsymbol{W}$	weight factor
C	weight coefficient
$\boldsymbol{x_i}$	*i*-th element of the *N*-dimension vector
$\boldsymbol{y_i}$	actual value, kW
m	the number of sampled buildings
j	one of sampled building
b	adjustable factor
ε	residual
ξ_i, ξ_i^*	training error
a_0,a_1,a_2	polynomial factors
t	time, h
$f(\boldsymbol{x_i})$	forecasting values, kW
$\varphi(\boldsymbol{x_i})$	feature space

all types of buildings can participate DR programs, while office buildings contribute to a large portion of DR reduction in practices, because their large volume. Thus, in our paper, office buildings are our study object. This does not mean that the SVR model only suitable for the office buildings. The general framework and the models work for other type of buildings as well.

Recently, several studies have introduced DR strategies [14–19]. While an important aspect of DR strategies concerns how performance should be measured, a key challenge relates to forecasting a fair and accurate baseline. A DR baseline is an estimate of the electricity that would be consumed by a customer in the absence of a DR program. Such baselines are a challenging aspect of DR programs, as they must represent what a load would be if a customer were to not apply curtailment measures.

DR performance is calculated as the difference between the baseline and actual load during a DR event. Customers' compensation depends on the amount of electricity demand reduction during DR events, as show at Fig. 1. This figure serves as an example of a DR baseline and of DR reduction. Typically, a DR event lasts for only a few hours on the hottest/coldest day, and thus the DR baseline as a short-term load forecasting measure differs from other long-term load forecasting mechanisms such as building energy-saving retrofitting and energy efficiency benchmarking.

In commercial DR applications, electricity loads and ambient temperatures before the DR events and real-time ambient weathers during DR event can be acquired from the DR platform. Thus, a real-time forecasting method that uses the historic data as input parameters is feasible. Because a large number of customers take part in a DR at the same time, a fast and accurate online method to forecast DR baselines and calculate the actual reductions for every customer is needed. For example, accurate baselines support the fair compensation of DR program participants, and particularly of those who pay directly for load reductions. Besides, such baselines also serve as useful information for resource planners and systems operators who wish to employ DR programs. Thus, a key question concerning DR pertains to how baselines must be determined. A generic and high accuracy method to calculate the baseline is imperative. The motivation of this paper is proposed a generic method to forecast a more accurately and fair baseline in DR programs.

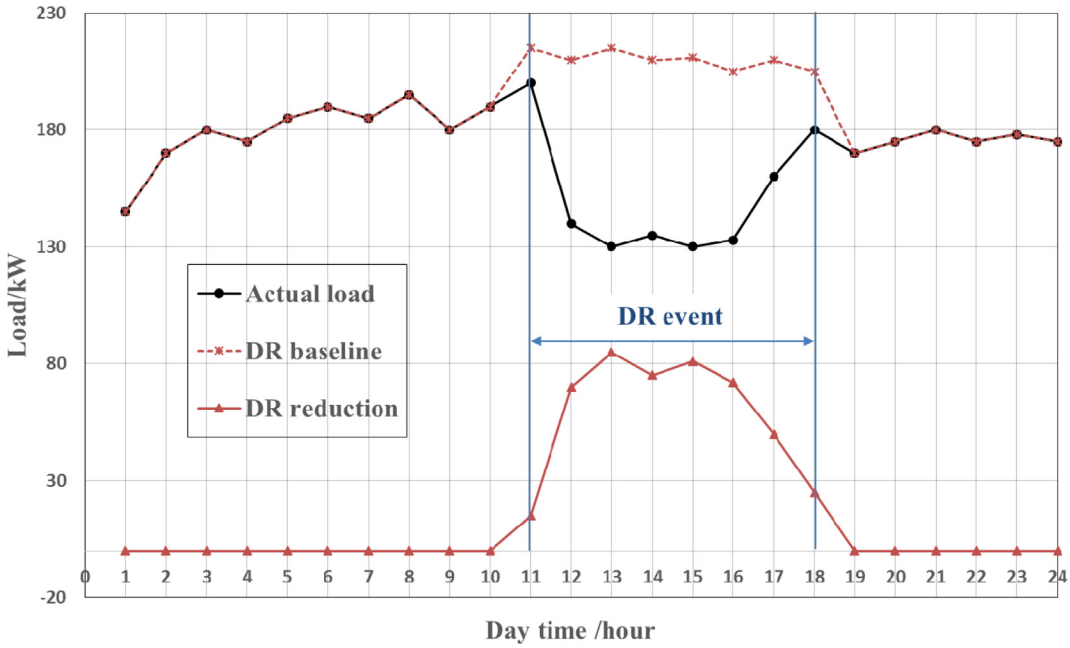

Fig. 1. Schematic of demand response baseline and reduction.

1.2. Existing load forecasting research

Several studies have been conducted on electric load forecasting. Guo-Feng Fan et al. presented a SVR model hybridized with the differential empirical mode decomposition (DEMD) method and with auto regression (AR) for electric load forecasting [20]. Similarly, Boroojeni KG et al. proposed a novel method to forecast power demand based on auto regression integrated moving-average model (ARIMA) [21–23]. Srivastav A et al. presented a novel approach to Gaussian Mixture Regression (GMR) for modeling building energy baselines via parameterized and locally adaptive uncertainty quantification [24]. These two methods require the use of complex algorithm models to calculate baselines, and they can be used to predict long-term loads as well.

Huilong Wang et al. used a multiple linear regression algorithm with classified load data from a sub-metering platform to calculate baselines. The authors showed that predicted sub-metering data can improve the accuracy of forecasts [25]. Ying Ji et al. proposed an "RC-S" model for estimating hourly cooling loads in commercial buildings using electricity sub-metering data [26]. Sub-meter systems are being used increasingly more often in buildings to separate out loads of air conditioning, lighting, power, or other equipment in buildings. Air conditioning loads are sensitive to weather conditions while light and other equipment are not. With sub-metering data, it is easy to predict whole building loads by distinguishing between weather sensitivity loads (air conditioning loads) and total loads. Xiwang Li and Jin Wen proposed a means of developing building energy estimation models for online building control and optimization using a system identification approach, and they concluded that this model can achieve 95% forecasting accuracy under one second intervals for small buildings and 88% accuracy for mid-sized office buildings [27].

The PJM Load Management Task Force [28] has conducted several DR baseline studies, analyzing a total of 11 baseline models with load additive adjustment, load ratio adjustment, weather sensitive adjustment and no adjustment, resulting in up to 44 different baselines included in the analysis. The results show that an appropriate baseline should consider empirical analysis results, expected administrative costs, and any other known issues based on previous practical experience (e.g., strategic behaviors) to maximize baselines and the applicability of baselines for customers that frequently respond. Goldberg ML. et al. examined a number of methods used by utilities and electrical system operators across United States and evaluated them in terms of accuracy and bias levels. They defined baseline calculation methods based on three fundamental components: a set of data selection criteria, an estimation method, and an adjustment method [29].

However, DR baselines require simple forecasting models, and models must be generic and thus specific building simulation models are not allowed. Otherwise, utility companies cannot use them in their DR programs. Some progress in simple methodological development has been achieved. Coughlin K et al. analyzed non-residential building baseline models, classified buildings into four types with different degrees of load variability and weather sensitivity, and found that the accuracy of baseline load models can be improved substantially by applying morning adjustments to all sampled buildings [30]. A White Paper [31] concluded that for most peak load management applications, high X of Y baselines with day-of adjustments create an optimal balance between accuracy, simplicity, and integrity. Kissock JK and Eger C built a multi-variable change-point model that measures industrial energy savings, and this model takes into account weather and production changes, and it is able to disaggregate savings into weather-dependent, production-dependent and independent components [32].

The above described forecasting models still present some deficiencies in terms of the short-term load forecasting of DR from predecessors. For example, researchers [20] have considered combinations of two algorithm models, which are too complex for utility companies to use. Researchers [2,28,30–32] have also used the average method based on historical data, which presents a degree of prediction accuracy when the load is relatively stable, but when the load is not stable, results are not very good. Finally, researchers [25,26] have used sub-metering data, which can improve prediction accuracy levels but which require sub-meter installation.

In recent years, Support Vector Regression (SVR) models have been used for load forecasting. SVR algorithms perform well in time series and nonlinear prediction. European Network on Intelligent Technologies for Smart Adaptive Systems hosted a global short-term load intelligent prediction contest in 2001. A team from Taiwan University that used the SVR algorithm won the contest [33].

In this paper, we propose a new SVR based method for calculating DR baselines. The SVR model proposed in this paper does not require the use of sub-metering data, as only historic electric load and weather data are needed. The method is generic, so specific building information is not needed. The SVR model offers a higher level of prediction accuracy and can achieve rapid computer calculation due to its simplicity. General speaking, this SVR model is useful to all DR participants. DR customers, can know whether the actual DR reduction is higher or lower than the anticipated reduction so that they can take some measures in advance. The planners can use the model to estimate the aggregated DR reduction of all customers. Thus, they can make reasonable policies in the power grid markets which integrated with more intermittent energy like solar and wind.

We selected workday electricity load data from July 23, 2014, to August 5, 2014, for four large commercial office buildings as our training sample dataset, and we collected data from 9 AM to 5 PM as a test dataset for August 6, 2014. The two-hour averaged dry-bulb temperature before DR is used as the temperature variable in the SVR model. The results show that this time window is the best in terms of DR forecasting accuracy.

This paper presented the selected criteria that ambient dry-temperature several hours before DR and verified two hours before is the best, this results could be a reference for other prediction models in office buildings and other different building types. This novel method has higher prediction accuracy and more stability compared with the existing methods in the DR programs nowadays. Furthermore, this generic approach can be easily extended to more homogenous building environment. We provided a detailed description of this innovative methodology compared with other existing methods, in this paper, we validated all of these models using four different office buildings.

The remainder of this paper is organized as follows. In Section 2, we introduce Support Vector Regression theory and other forecasting methods. In Section 3, we describe the SVR model developed and methodological development involved in the SVR model, the data source, building load impact factors and the baseline evaluation method. In Section 4, we describe each forecasting model investigated in this paper and the corresponding results. In Section 5, we present our conclusions and avenues for future research.

2. Methodology

2.1. Support Vector Regression (SVR)

SVR constitutes a new and promising approach to data regression. SVR principles for regression are as follows. Given a dataset of $\overline{N}$ elements $\{(\mathbf{X}_i, \mathbf{y}_i) i = 1, 2, \ldots \overline{N}\}$, N denotes samples in the training dataset, $\mathbf{X}_i$ is the i-th element of the N-dimension vector, *i.e.*, $\mathbf{X}_i = \{x_1, x_2, \ldots x_n\} \in R^n$, and $\mathbf{y}_i \in R$ is the actual value corresponding to $\mathbf{X}_i$.

In SVR, by mapping training data $\mathbf{X}_i$ into the high l -dimensional feature space, this feature space formulates an optimized hyperplane that also represents the non-linear relationship between input (independent variables) and output data (dependent variables). This is the SVR function, which is written as Eq. (1).

$$f(\boldsymbol{x}) = \boldsymbol{W}^T \varphi(\boldsymbol{x}) + b \tag{1}$$

where $f(\boldsymbol{x})$ denotes the forecasting values, $\boldsymbol{W}$ is the l-dimensional weight factor, b is the adjustable factor, and $\varphi(\boldsymbol{x})$ is the map function of mapping $\mathbf{X}_i$ into the high l-dimensional feature space.

Here, introduce the ε insensitive loss function defined as Eq. (2).

$$|y - f(\boldsymbol{x})|_\varepsilon = \max(0, |y - f(\boldsymbol{x})| - \varepsilon) \tag{2}$$

Define the residual between the actual value y and forecasting value $f(\boldsymbol{x})$ using Eq. (3).

$$R(x, y) = y - f(\boldsymbol{x}) \tag{3}$$

The ideal regression includes the full residual within a range of ε as shown in Eq. (4).

$$-\varepsilon \leqslant R(x, y) \leqslant \varepsilon \tag{4}$$

The hypothesis for the entire training dataset satisfies Eq. (4). Thus, the data are farthest from the hyperplane when the residual is satisfied with $R(x, y) = \pm\varepsilon$. The distance between data (x, y) and the hyperplane $R(x, y) = 0$ is defined as $|R(x, y)|/\|W^*\|$, and W^* is defined as Eq. (5).

$$W^* = (1, -\boldsymbol{W}^T)^T \tag{5}$$

We hypothesize that the maximum distance between the data (x, y) and hyperplane $R(x, y) = 0$ is δ. Thus, all training data are satisfied by Eq. (6). Maximizing δ means that the SVR model offers maximum generalization capacity.

$$|R(x, y)| \leqslant \delta \|W^*\| \tag{6}$$

A maximum distance is reached when $|R(x, y)| = \varepsilon$, and thus Eq. (6) can be rewritten as Eq. (7). To maximize δ, $\|W^*\|$ should be a minimum value, and $\|W^*\|^2 = \|W\|^2 + 1$ with the optimization issue changing to a minimum $\|W\|$.

$$\varepsilon = \delta \|W^*\| \tag{7}$$

However, some training errors may exceed the $(-\varepsilon, \varepsilon)$ region, and training errors of less than $-\varepsilon$ are denoted as ξ_i whereas a training error exceeding ε is denoted as ξ_i^*. ξ_i and ξ_i^* are defined as Eqs. (8) and (9), respectively. A schematic of ξ_i and ξ_i^* is shown in Fig. 2.

$$\xi_i = \begin{cases} 0 & R(x_i, y_i) - \varepsilon \leqslant 0 \\ R(x_i, y_i) - \varepsilon & others \end{cases} \tag{8}$$

$$\xi_i^* = \begin{cases} 0 & \varepsilon - R(x_i, y_i) \leqslant 0 \\ \varepsilon - R(x_i, y_i) & others \end{cases} \tag{9}$$

The SVR focuses on finding the optimum hyperplane and minimizing the training error between training data and the ε insensitive loss function. Therefore, the SVR optimization objective function is written as Eq. (10).

$$\min F(W, b, \xi_i, \xi_i^*) = \frac{1}{2}\|W\|^2 + C\sum_{i=1}^{N}(\xi_i + \xi_i^*) \tag{10}$$

with the constraints:

$$y_i - \boldsymbol{W}^T \varphi(\boldsymbol{x_i}) - b \leqslant \varepsilon + \xi_i \quad i = 1, 2, \ldots, \overline{N}$$
$$\boldsymbol{W}^T \varphi(\boldsymbol{x_i}) + b - y_i \leqslant \varepsilon + \xi_i^* \quad i = 1, 2, \ldots, \overline{N}$$
$$\xi_i \geqslant 0, \xi_i^* \geqslant 0 \quad i = 1, 2, \ldots, \overline{N}$$

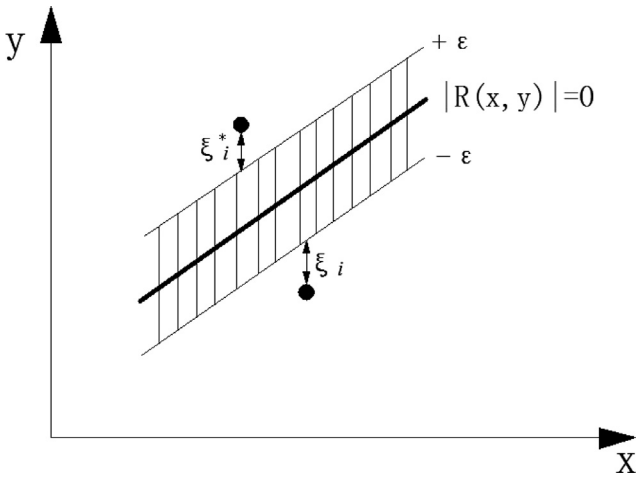

Fig. 2. Schematic of ξ_i, ξ_i^*, $-\varepsilon$, $+\varepsilon$.

where C is the parameter that trades off training errors and the maximum distance between training data and the hyperplane space. The first term of Eq. (10) is used to penalize large weights to maintain regression function flatness, and the second term determines the balance between confidence and experience risk using the ε insensitive loss function.

After the quadratic optimization problem with inequality constraints is solved, the l-dimensional weight factor $\boldsymbol{W}$ in Eq. (1) is obtained as Eq. (11).

$$\boldsymbol{W} = \sum_{i=1}^{N}(\beta_i^* - \beta_i)\varphi(\boldsymbol{x_i}) \tag{11}$$

where β_i^* and β_i are obtained by solving a quadratic program and are the Lagrangian multipliers. Finally, the SVR regression function is written as Eq. (12).

$$f(\boldsymbol{x}) = \sum_{i=1}^{N}(\beta_i^* - \beta_i)K(\boldsymbol{x_i} - \boldsymbol{x}) + b \tag{12}$$

where $K(\boldsymbol{x_i} - \boldsymbol{x})$ is referred to as the kernel function, which is capable of nonlinearly mapping the training data into a high l-dimensional space. Thus, it is suited to addressing nonlinear relationship problems (e.g., electricity forecasting).

2.2. Other forecasting baselines

Several existing models focus on baseline load forecasting. These models include the historic data average model, the historic data average with morning adjustment method, the polynomial regression model, etc. All of these models offer differing degrees of prediction accuracy within specified limits [28–32]. Table 2 lists all of the forecasting models examined in this paper. These baseline models are explained below.

2.2.1. Baseline 1–3: M out of N baseline ($N \geqslant M$)

This baseline consists of hourly loads averaged across the "highest M out of N" most recent days with a selection criterion of the M highest load days out of the preceding N days, where the N excludes holidays and weekends. In this study, we selected three typical models including 4 out of 5 baseline (*BL-#1*), 10 out of 10 baseline (*BL-#2*) and 5 out of 10 baseline (*BL-#3*) to compare with our SVR baseline.

Table 1
Baseline adjustment algorithms.

Number	Type	Simplified algorithm	Pre-event hours
BL-#5	Load additive	PBL + [load(pre-event hours)-PBL(pre-event hours)]	2 pre-event hours
BL-#6	Load ratio	PBL * [load(pre-event hours)/PBL(pre-event hours)	2 pre-event hours

Note: in this table, PBL denotes the provisional predicted baseline, which uses historical data for calculations via the average method.

Table 2
Existing baseline models and the new SVR baseline.

Serial number	Forecasting models
BL-#1	4 out of 5 baseline
BL-#2	10 out of 10 baseline
BL-#3	5 out of 10 baseline
BL-#4	Middle 4 out of 6 baseline
BL-#5	5 out of 10 baseline (morning additive adjustment)
BL-#6	5 out of 10 baseline (morning ratio adjustment)
BL-#7	10 day dry-bulb temperature regression baseline
BL-#8	New SVR baseline (10 pre-event days)

2.2.2. Baseline 4: Middle M out of N baseline ($M = N - 2$)

The middle M out of the N baseline is similar to the M out of N baselines except that the selection criterion for comparison days involves dropping the lowest and highest load days out of the most recent N days with no holidays or weekends. We chose the middle 4 out of 6 (*BL-#4*) as the model to compare with our SVR model.

2.2.3. Baseline 5 & 6: M out of N morning adjustment baseline ($N \geqslant M$)

Two different baseline morning adjustment algorithms are considered in this evaluation method. One is the directed load additive adjustment, and the other is the load ratio adjustment. We chose 5 out of 10 as the morning adjustment model with no holidays or weekends. Table 1 provides a simplified overview of the two proposed adjustment methods.

2.2.4. Baseline 7: N days regression baseline

The N days regression baseline is calculated using a regression model consisting of a daily energy equation that uses the total electric load as the dependent variable and 24 hourly energy fraction equations. In each energy fraction equation, dependent variables constitute the fraction of the daily load occurring in each hour of a day. Independent variables in this model include work schedule variables and dry-bulb temperatures.

We chose the 10-day regression baseline type (*BL-#7*), with hourly loads averaged over 10 days to form the dependent variable and with the hourly dry-bulb temperature averaged over 10 days to form the independent variables. The polynomial fitting function is defined as Eq. (13).

$$y = a_0 + a_1 * x_T + a_2 * x_T^2. \quad (13)$$

where y is the dependent variable, which is standard hourly electricity loads. x_T denotes the independent variables, which is standard for hourly temperature. a_0, a_1 and a_2 are the polynomial factors.

3. SVR baseline model and methodological development

3.1. SVR model

In this study, we propose a short-term load forecasting method based on the SVR model. A set of historical data is used to train the model to determine the optimal function relationship between the input (independent variables) and output (dependent variables). We then use this optimal function to predict outcomes. An SVR model development and validation flow chart is shown in Fig. 3. This model only needs real-time weather data to forecast the DR baseline. The weather data is easily accessible from local meteorological agencies or field measurements. A case study of four office buildings is used to evaluate the proposed model and the result is promising.

3.2. Data source

We selected four large office buildings in eastern China as our target sample. They are referred to as Office_1, Office_2, Office_3 and Office_4 as showed in Table 3.

We collected electricity load data (data time interval of 15 min) for workdays from July 23, 2014, to August 6, 2014. The average value per hour was recorded in the dataset. As in several metering datasets, we found that a small amount of data were missing,

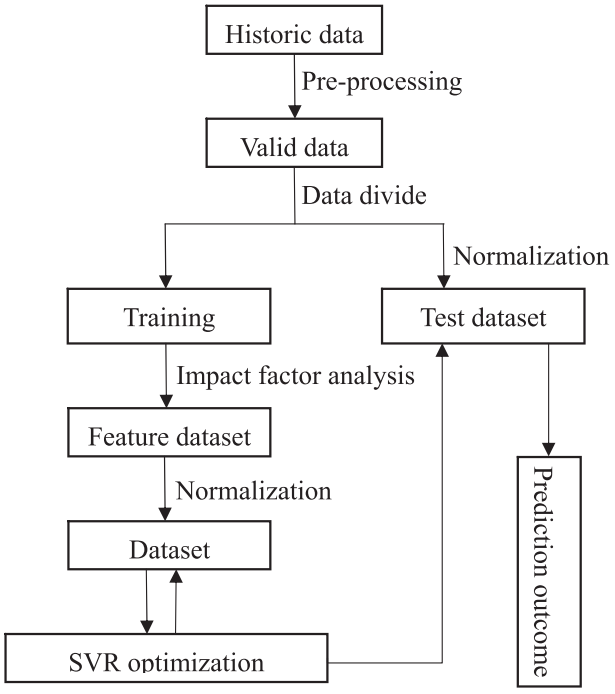

Fig. 3. SVR model development and validation flow chart.

Table 3
The detailed information of office buildings.

Office number	Floor area (m^2)	Occupancy rate (%)	HVAC system
Office_1	42,820	85	Chillers for summer cooling and steam heaters for winter heating
Office_2	45,000	95	Same as Office_1
Office_3	40,111	85	Variable refrigerant volume (VRV) units for cooling and heating
Office_4	32,000	95	Same as Office_1

potentially due to signal transmission failures or acquisition instrument malfunctions. The pre-processing of these missing data is necessary. For example, we employed a data interpolation method to calculate the hourly average load for missing Office_3 11:30 AM, July 31th data. The interpolation method is defined as Eq. (14):

$$D(t_m) = \frac{D(t-15') + D(t+15')}{2} \tag{14}$$

where $D(t_m)$ is the electricity load at time t_m, $D(t-15')$ is the electricity load 15 min before at time t_m, and $D(t+15')$ is the electricity load after 15 min at time t_m.

When more than two data points were missing for one hour, all data corresponding to that given hour were eliminated, and Eq. (15) was used to calculate the load:

$$D(t_h) = \frac{D(t-1) + D(t+1)}{2} \tag{15}$$

where $D(t_h)$ is the electricity load at time t_h, $D(t-1)$ is the electricity load before one hour at time t_h, and $D(t+1)$ is the electricity load after one hour at time t_h.

When more than two data points are missing over two consecutive hours, all data for that given day are eliminated. Fortunately, we did not experience this when analyzing our sample dataset.

The load profile after data processing is shown in Fig. 4. In our analysis of the SVR, we removed the weekend day load from the model so that it did not include the weekend electricity load. DR programs are usually applied for the hottest summer day. Therefore, we used August 6th as the DR event day. Weather data were collected from the local weather bureau, and weather files mainly include dry bulb temperatures, dew point temperatures, pressure levels, etc. Only dry bulb temperatures are used here.

3.3. SVR method development

The electricity loads of office buildings can be influenced by several factors, including ambient parameters, electrical equipment, working hours, etc. Therefore, there are many optional independent variables in the SVR forecast model. In this study, to easily calculate baselines, we use weather parameters and building working schedules as independent variables in the SVR model, as these two variables are easy to obtain from DR programs. We use the work schedule factor to reflect changes in building electricity consumption. Furthermore, the EnergyPlus software program was used to simulate the weather parameter's influence on electricity consumption. These two independent variables are validated as follows.

3.3.1. Working schedule factor

Working schedule factors referenced here mainly include the times at which occupants come and leave. For the four office buildings examined, working hours run from 9:00 AM to 17:00 PM. Fig. 5 shows the load profiles of four office buildings for August 6, 2014. The figure shows that the work load began to increase two hours before working time and reached a stable value at 9:00. We also found that the increments for each building vary, Office_2's increment is the most abrupt while Office_4 and Office_3's increments are more gradual. The load increments of each building are shown in Table 4. Likewise, most electrical equipment was turned off at 17:00 PM, causing electricity loads to decline. We conclude that working schedules critically affect electricity loads in different buildings.

3.3.2. Weather factor

We use EnergyPlus to establish a simulation office building. This building model is based on the Chinese Design Standard for the Energy Efficiency of Public Buildings. The standard requirement is very similar to ASHRAE 90.1 [34]. The main input parameter settings in EnergyPlus IDF files are illustrated in Table 5. The total load demand for buildings is calculated separately under different meteorological parameters, where temperature parameter settings for each model are illustrated in Table 6. In keeping other parameters constant in EnergyPlus while only changing weather parameters (dry bulb temperature), we obtained the building load profile from 8am to 6 pm, which is shown in Fig. 6. From this figure, we can find that when the dry-temperature increase a small little proportion (e.g. 10%), the total electricity load of the modeling building increased nearly 20%. It can be concluded that building electricity loads increase as outdoor dry bulb temperature is augmented, which is also an important factor affecting building electricity loads, thus, we choose the dry-temperature as one of key impact factor in our SVR model.

Furthermore, building construction and furniture constitute cold/hot thermal storage mass, and this stored energy is released when ambient temperatures change to act as a temperature buffer (i.e., "thermal inertia"). Thermal inertia is defined by Ferrari S as the heat storage capacity of a building structure and as its performance in delaying heat transmission [35]. The thermal storage mass delays ambient temperature effects on building interior temperatures, delaying weather sensitive equipment electricity con-

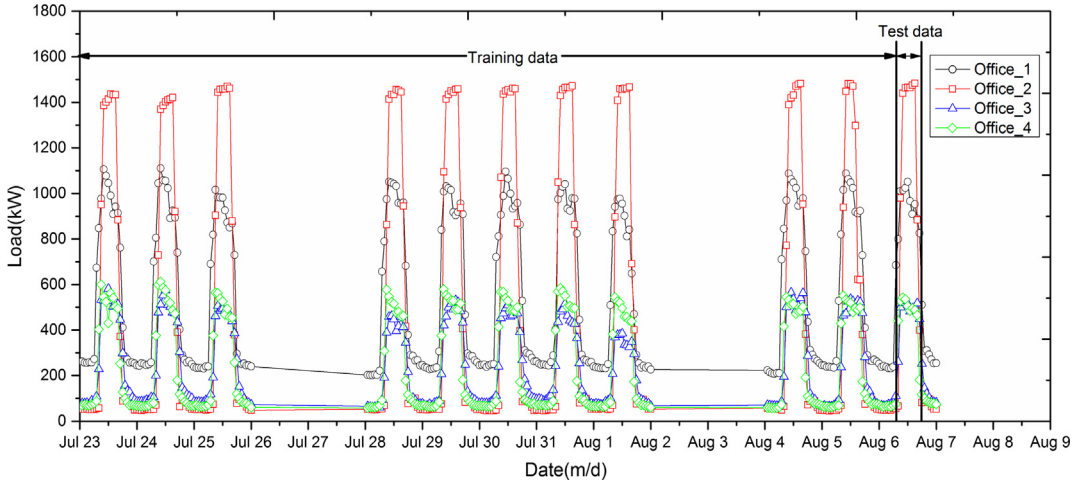

Fig. 4. Historic hourly electricity load profile.

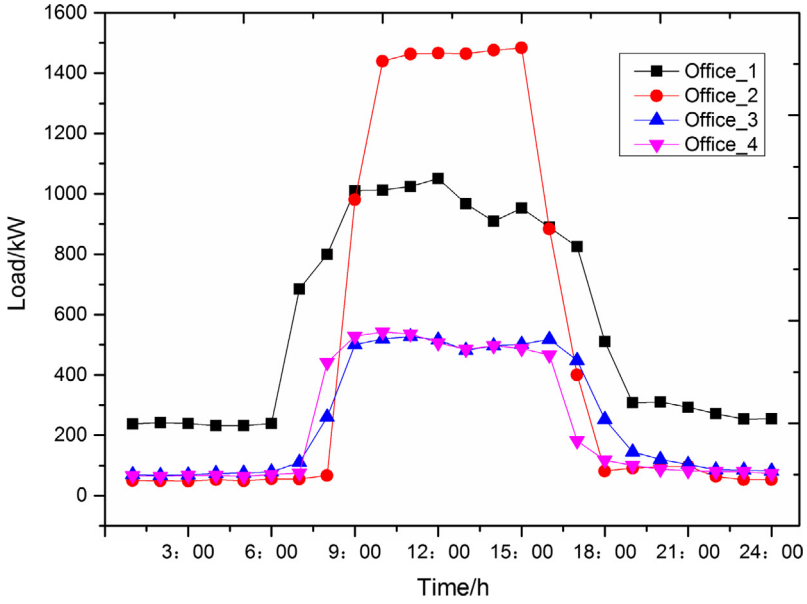

Fig. 5. Electricity load profile for August 6, 2014.

Table 4
Pre-event load increments of the four buildings studied.

Building NAME	7:00 to 8:00 AM	8:00 to 9:00 AM	Average
Office_1	17%	26%	22%
Office_2	22%	1372%	697%
Office_3	136%	92%	114%
Office_4	488%	20%	254%

sumption. To improve the accuracy of the SVR forecast model, we selected pre-event outdoor dry bulb temperature variables, including six conditions: SVR real-time temperature (real-time T), SVR pre-one-hourly average temperature (pre-one AT), SVR pre-two-hourly average temperature (pre-two AT), SVR pre-three-hourly average temperature (pre-three AT), SVR pre-four-hourly average temperature (pre-four AT) and SVR pre-six-hourly average temperature (pre-six AT). We used electricity usage data for the four office buildings for our analysis. The corresponding results are shown in Table 7.

Table 7 shows that using the pre-event temperature can improve prediction accuracy levels, and the pre-two AT model is the most accurate. We use this forecasting model in the following prediction.

From the above analysis, we conclude that working time and outside dry bulb temperatures heavily influence the building electricity load. Thus, they were selected as independent variables, and electricity load was used as a dependent variable. Table 8 presents the training and test dataset of the SVR model (*BL-8#*).

In Table 8, x_1 denotes the dry bulb temperature, x_2 denotes the daily time, y_1 denotes the forecasting load, i denotes the day, j

Table 5
Building information settings used in EnergyPlus.

Input parameters	Value	Input parameters	Value
Exterior wall heat transfer coefficient	0.97 W/(m^2 K)	Infiltration wind	1ACH
Roof heat transfer coefficient	0.346 W/(m^2 K)	Lighting	12 W/m^2
Window heat transfer coefficient	2.5 W/(m^2 K)	Equipment	15.7 W/m^2
Shading coefficient	0.4	Air conditioning	VRV
Building/air conditioning area	3800 m^2		

Table 6
Outdoor dry-bulb temperature settings used in EnergyPlus.

Time (h)	Model_T1 (°C) (real-time)	Model_T2 (°C) (10% increments)	Model_T3 (°C) (20% increments)	Model_T4 (°C) (30% increments)
8:00	25.3	27.8	30.4	32.9
9:00	26.2	28.8	31.4	34.1
10:00	27.1	29.8	32.5	35.2
11:00	28.0	30.8	33.6	36.4
12:00	28.8	31.7	34.6	37.4
13:00	29.5	32.5	35.4	38.4
14:00	30.0	33.0	36.0	39.0
15:00	30.3	33.3	36.4	39.4
16:00	30.4	33.4	36.5	39.5
17:00	30.1	33.1	36.1	39.1
18:00	29.4	32.3	35.3	38.2

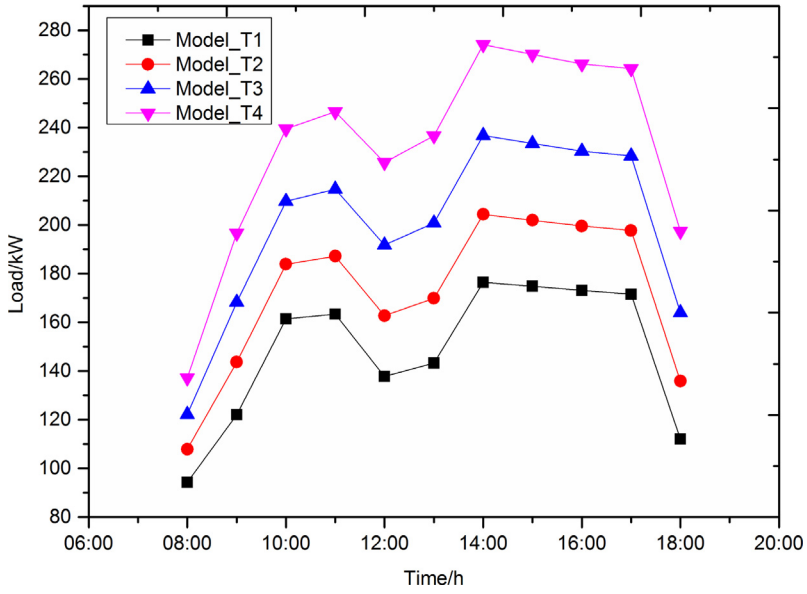

Fig. 6. Electricity load profiles based on different temperature models.

Table 7
Predicted mean errors of the different models.

Building	Real-time T	Pre-one AT	Pre-two AT	Pre-three AT	Pre-four AT	Pre-six AT
Office_1	1.77%	1.89%	−0.62%	0.42%	1.02%	−0.84%
Office_2	5.67%	−1.90%	1.52%	1.85%	3.28%	2.65%
Office_3	6.28%	3.2%	2.05%	1.31%	1.04%	2.17%
Office_4	−3.41%	−1.55%	−2.08%	−2.75%	−3.12%	−5.29%
MAE	**4.28%**	**2.14%**	**1.57%**	**1.58%**	**2.12%**	**2.74%**

Table 8
Training and test dataset.

Variables	Symbol	Dataset category	The range of i and j
$\boldsymbol{x}_1$	$T(d_i t_j)$	Training dataset	$(i = 1,\ldots 11; j = 1,\ldots 24)$
$\boldsymbol{x}_2$	H_{ij}		when $i = 11; j = 1,\ldots 8$
$\boldsymbol{y}_1$	$P(d_i t_j)$	Test dataset	$(i = 11; j = 9,\ldots 17)$

denotes the hour corresponding to a given day, $T(d_i t_j)$ denotes the dry bulb temperature recorded during the j hour corresponding to the i day, H_{ij} denotes the hour, $P(d_i t_j)$ denotes the forecasting load recorded during the j hour corresponding to the i day.

This novel SVM method aim at DR programs short time baseline forecast. In our study, we choose the real office buildings' electricity data of ten days before the DR event (a virtual DR event from 9 am to 5 pm) as training dataset, then predicted the eight hours electricity load during the DR event. There are 248 training data points, eight test data points to validate the SVM predicted model and concluded. This baseline is up to eight hours, thus, the novel forecast methods is suitable to most of the office buildings' DR programs nowadays which usually continually two to four hours.

3.4. Forecasting evaluation methods

Load forecasting involves the estimation of future loads. The difference between the estimated future load and actual load is the prediction error. This paper focuses on short-term DR electricity load forecasting, as DR participants are more concerned with the gap between the baseline and actual load during a DR event. The absolute error (AE), mean error (ME) and mean absolute error (MAE) during a response time are taken as evaluation standards of prediction accuracy in this paper, and evaluation methods are expressed as Eqs. (16)–(18):

$$AE(t_i) = D(t_i) - P(t_i)\ (i = 1, 2, \ldots n) \tag{16}$$

$$ME = \frac{\sum_{i=1}^{n}[D(t_i) - P(t_i)]}{\sum_{i=1}^{n} D(t_i)} \times 100\%\ (i = 1, 2, \ldots n) \tag{17}$$

$$MAE = \frac{\sum_{j=1}^{m}\left|\frac{\sum_{i=1}^{n}[D(t_i)-P(t_i)]}{\sum_{i=1}^{n} D(t_i)} \times 100\%\right|}{m}\ (i = 1, 2, \ldots n; j = 1, 2, \ldots m) \tag{18}$$

where $D(t_i)$ is the actual load at time t_i, $P(t_i)$ is the prediction load at time t_i, n is the number of hours for the forecasting period, t_i denotes the time i, m is the number of sampled buildings, and j represents one sampled building.

4. Comparison between the new baseline method and existing methods

We applied the eight load baseline forecasting models (Table 2) to the four office buildings, and we compared prediction load results with the actual load to determine the forecasting accuracy of these models. The predictive results of the four office buildings during a virtual DR event from 9 am to 5 pm are shown in Figs. 7–10, the detailed information of this four office buildings as depicted in Table 3. The prediction mean error is listed in Table 9.

It can be seen from Fig. 7 that the accuracy of all eight models is acceptable. The mean error of BL-#8 is −0.62%, which is the best. The worst one is BL-#3 with −1.28% of the mean error, which is

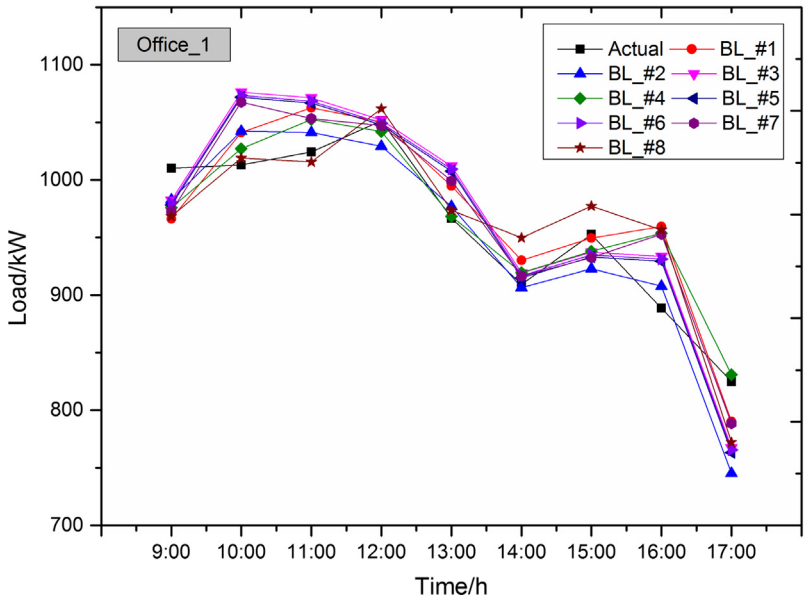

Fig. 7. Load prediction profile of Office_1.

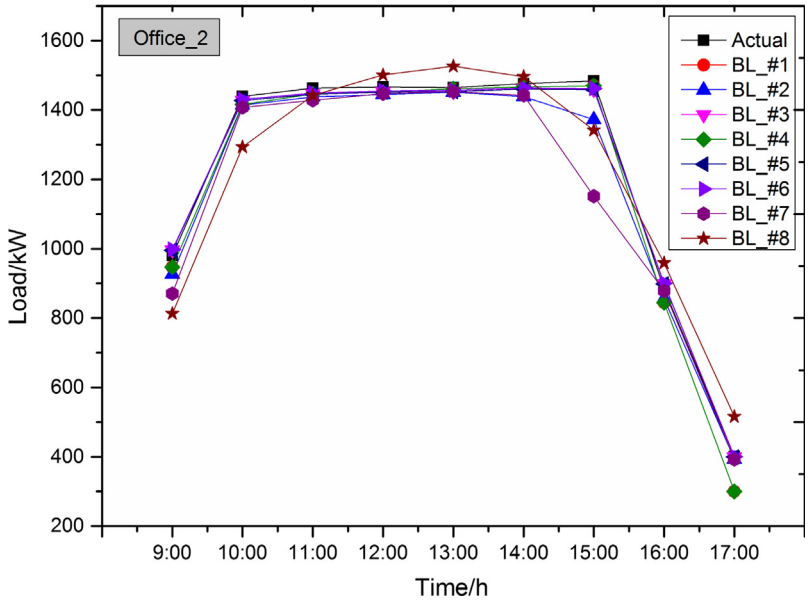

Fig. 8. Load prediction profile of Office_2.

also acceptable. The prediction results are all close to the actual loads. Fig. 8 shows that the curve of the *BL-#8* model is smoother, and predicted load of the *BL-# 8* model tends to fluctuate around the actual value, the same results can be found in other three figures. For the BL-#5 and BL-#6 with morning adjustment, the prediction result is very close to the actual load with the mean error is 0.60% and 0.36% respectively. However, Figs. 9 and 10 present morning adjustment model (BL-#5, BL-#6) is the least accuracy, especial for the BL-#6 model in office_3 with the mean error up to −20.08%. For the historical data average models (BL-#1 ~ BL-#4) without morning adjustment, the prediction accuracy is acceptable.

Positive values in Table 9 indicate that a prediction value is less than the actual value, and negative values indicate that a prediction value is larger than the actual value. Table 9 indicates the prediction trend is nearly consistent in different models, as shown in office_1, office_2 and office_4. The prediction results are either higher or lower than the actual loads. Also, this table shows that the *BL-#8* prediction model does not always offer the highest level of prediction accuracy for all buildings sampled. For example, the ME of the *BL-#8* model for Office_1 building is −0.62% which is lowest value, the ME of the *BL-#7* model for Office_3 is the lowest at 1.55%, the *BL-#4* model presents the lowest ME value of −2.02% for Office_4, and the *BL-#6* prediction model offers better performance for Office_2. For the *BL-#5* and *BL-#6* models with morning adjustments, the prediction accuracy of Office_1 and Office_2 is satisfactory while the results for Office_3 and Office_4 are the worst. The *BL-#7* model offers satisfactory prediction accuracy levels for Office_3, Office_1 and Office_4, but it presents the lowest degree of accuracy for Office_2. We can thus conclude that the *BL-#8* model generated the best results among the buildings examined.

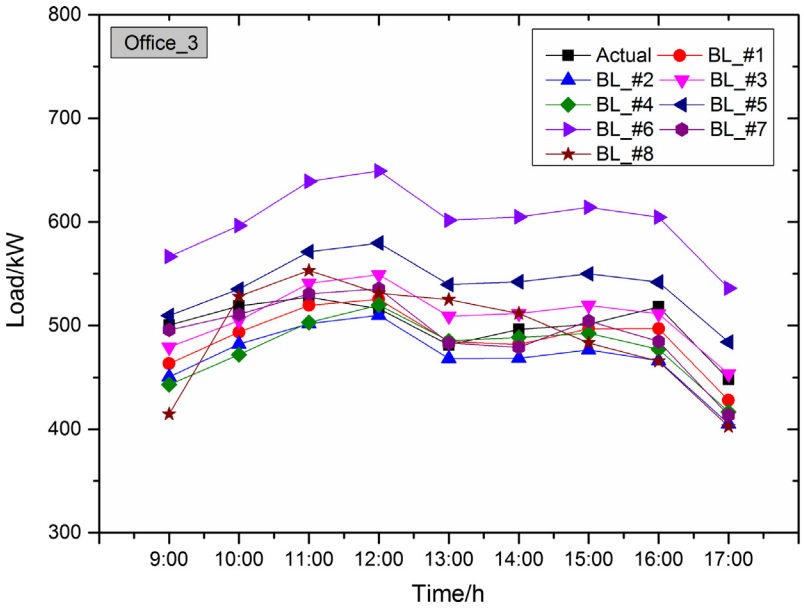

Fig. 9. Load prediction profile of Office_3.

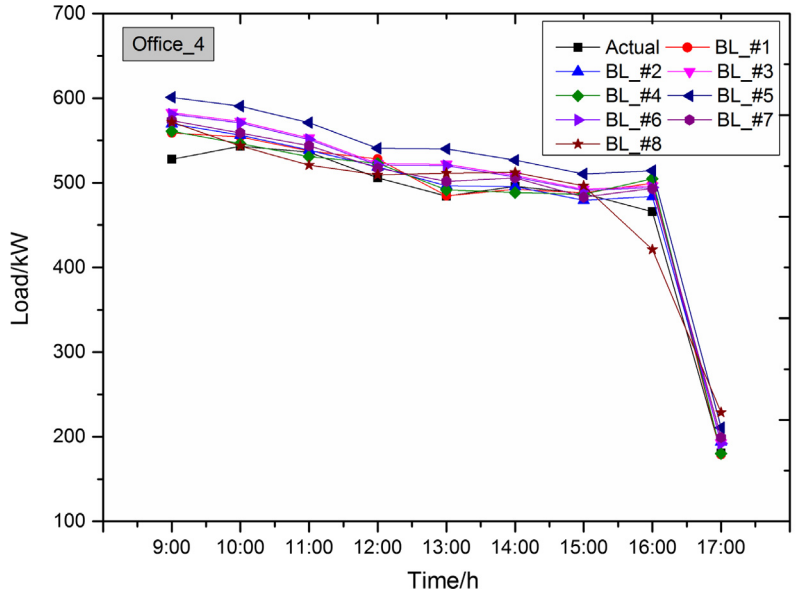

Fig. 10. Load prediction profile of Office_4.

Table 9
Predicted mean error (ME) of the four commercial buildings.

Building	BL-#1	BL-#2	BL-#3	BL-#4	BL-#5	BL-#6	BL-#7	BL-#8
Office_1	−1.20%	1.00%	−1.28%	−0.78%	−0.83%	−1.02%	−1.04%	−0.62%
Office_2	2.30%	2.91%	0.57%	2.30%	0.60%	0.36%	5.30%	1.52%
Office_3	2.61%	6.19%	−1.58%	4.66%	−7.67%	−20.08%	1.55%	2.05%
Office_4	−2.26%	−2.48%	−5.10%	−2.02%	−8.95%	−4.76%	−3.53%	−2.08%
MAE	**2.09%**	**3.15%**	**2.13%**	**2.44%**	**4.51%**	**6.56%**	**2.86%**	**1.57%**

In addition, while analyzing MAE, we found that the *BL-#8* model is the most accurate, but the *BL-#1*, *BL-#3*, *BL-#4* and *BL-#7* models offer satisfactory results as well. We also found from Figs. 7–10 that not all prediction data points of the *BL-# 8* model present the highest levels of prediction accuracy, and occasionally, its deviation from the actual load is larger than that of other models as shown in Fig. 8. According to Figs. 9 and 10, the *BL-#5* and *BL-#6* models present higher values than the actual value, indicating that the two models are not suitable for Office_3 and Office_4 and that these models must categorize buildings to attain higher levels of forecasting accuracy. The above analysis shows that the *BL-#8* model offers the highest degree of forecasting

accuracy and that this model offers the most stable performance for all four buildings examined.

5. Conclusions and future work

This paper proposes a new SVR method based on forecasting models for calculating DR baselines of office buildings. A new ambient temperature forward selected method are proposed in this model. We compared the SVR forecasting model with the other seven traditional forecasting models are used to calculate the DR baselines. These seven models mainly include the simple average model with historical data, the average model combined with morning adjustments, and the outdoor dry bulb temperature polynomial regression model.

We draw the following conclusions from this study. In this novel SVR model we take the dry bulb temperature several hours before the DR event as the temperature independent variable. For office buildings, the MAE of real-time, pre-one, pre-two, pre-there, pre-four and pre-six hours is 4.28%, 2.14%, 1.57%, 1.58%, 2.12% and 2.74% respectively, take dry bulb temperature pre-two hours can improve the forecasting accuracy best. The accuracy of the SVR model in forecasting the DR baseline of office building is much better than traditional calculated methods, the MAE of SVR model is 1.57% in our four office building examples is the best. Compared to other seven models the model is very generic and can be applied to a wide variety of office buildings, the ME of our four office building examples is −0.62%, 1.52%, 2.05% and −2.08% respectively, these predicted accuracy are more stable, and the predicted profile of SVR model tends to be smooth, causing its prediction value to fluctuate around the actual value. With morning adjustment models like BL-#5 and BL-#6 its prediction results are unstable, for BL-#6 model, the ME of Office_2 is 0.36%, however the ME of Office_3 is up to −20.08%. Although these models are hottest in DR baseline forecasting and offer a higher degree of prediction accuracy under the building conditions classified in previous studies, we do not think they serve as good generic method for improving DR baselines.

The SVR model proposed in this paper is suitable for real-time calculation, to expend the application and improve its efficiency, this methodology will be made into a prototype toolkit in future studies. And this toolkit can also be integrated in energy management system or DR control platform to calculate the DR baseline online.

We believe that SVR models can be used by utilities professional for baseline calculation in DR programs. However, this paper only predicted the DR baseline for eight hours on working days, some DR events may be shorter, and model prediction accuracy levels may vary. In addition, only office building electricity loads are forecasted in this paper while other buildings such as residential and industrial buildings are not studied. As the structures and thermal masses of such buildings vary, the temperature advance time may vary as well. Finally, other independent variables such as occupancy rates, electricity price and building types in the model should be cover, not all situations are analyzed here, and so more detailed conclusions will require comprehensive analysis in the future. Additional studies are needed to build a reliable forecast baseline for different types of buildings commonly used in DR events.

Acknowledgement

This material is based upon work supported by China National Grid Company Technology Foundation under Grant# SGZJ0000BGJS1500460.

References

[1] Federal Energy Regulation Commission. 2010 assessment of demand response and advanced metering. Washington DC: United States Department of Energy; 2011.
[2] Barton J, Huang S, Infield D, Leach M, Ogunkunle D, Torriti J, et al. The evolution of electricity demand and the role for demand side participation, in buildings and transport. Energy Policy 2013;52:85–102.
[3] Critz DK, Busche S, Connors S. Power systems balancing with high penetration renewables: the potential of demand response in Hawaii. Energy Convers Manage 2013;76:609–19.
[4] Mathiesen BV, Dui N, Stadler I, Rizzo G, Guzovi Z. The interaction between intermittent renewable energy and the electricity, heating and transport sectors. Energy 2012;48:2–4.
[5] Alimohammadisagvand B, Jokisalo J, Kilpelainen S, Ali M. Cost-optimal thermal energy storage system for a residential building with heat pump heating and demand response control. Appl Energy 2016;174:275–87.
[6] Broeer T, Fuller J, Tuffner F, Chassin D, Djilali N. Modeling framework and validation of a smart grid and demand response system for wind power integration. Appl Energy 2014;113:199–207.
[7] Lorenzi G, Silva CAS. Comparing demand response and battery storage to optimize self-consumption in PV systems. Appl Energy 2016;180:524–35.
[8] Babonneau F, Caramanis M, Haurie A. A linear programming model for power distribution with demand response and variable renewable energy. Appl Energy 2016;181:83–95.
[9] Magnago FH, Alemany J, Lin J. Impact of demand response resources on unit commitment and dispatch in a day-ahead electricity market. Int J Electr Power Energy Syst 2015;68:142–9.
[10] Bartusch C, Alvehag K. Further exploring the potential of residential demand response programs in electricity distribution. Appl Energy 2014;125:39–59.
[11] Cappers P, Goldman C, Kathan D. Demand response in U.S. electricity markets: empirical evidence. Energy 2010;35:1526–35.
[12] Torriti J, Hassan MG, Leach M. Demand response experience in Europe: policies, programs and implementation. Energy 2010;35:1575–83.
[13] Shen B, Ghatikar G, Lei Z, Li JK, Wikler G, Martin P. The role of regulatory reforms, market changes, and technology development to make demand response a viable resource in meeting energy challenges. Appl Energy 2014;130:814–23.
[14] Sehar F, Pipattanasomporn M, Rahman S. An energy management model to study energy and peak power savings from PV and storage in demand responsive buildings. Appl Energy 2016;173:406–17.
[15] Patteeuw D, Bruninx K, Arteconi A, Delarue E, Dhaeseleer W, Helsen L. Integrated modeling of active demand response with electric heating systems coupled to thermal energy storage systems. Appl Energy 2015;151:306–19.
[16] Weilin L, Peng X. A fast method to predict the demand response peak load reductions of commercial buildings. Sci Technol Built Environ 2016.
[17] Weili L, Peng X, Feifei J. Optimal demand response strategy of a portfolio of multiple commercial buildings: methods and a case study. Sci Technol Built Environ 2016.
[18] Amini MH, Frye J, Ilic MD, Karabasoglu O. Smart residential energy scheduling utilizing two stage mixed integer linear programming. In: IEEE 47th North American power symposium. Oct. 4–6; 2015 [in USA].
[19] Kamyab F, Amini MH, Sheykhha S, Hasanpour M, Jalali MM. Demand response program in smart grid using supply function bidding mechanism. IEEE Trans Smart Grid 2016;7:1277–84.
[20] Fan Guo-Feng, Peng Li-Ling, Hong Wei-chiang, Sun Fan. Electric load forecasting by the SVR model with differential empirical mode decomposition and auto regression. Neurocomputing 2016;173:958–70.
[21] Boroojeni KG, Mokhtari S, Amini MH, Iyengar SS. Optimal two-tier forecasting power generation model in smart grids. Int J Informat Process 2014;8:79–88.
[22] Boroojeni KG, Amini MH, Bahrami S, Iyengar SS, Sarwat AI, Karabasoglu O. A novel multi-time-scale modeling for electric power demand forecasting: from short-term to medium-term horizon. Electric Power Syst Res 2017;142:58–73.
[23] Amini MH, Moghaddam P, Forushani EH. Forecasting the PEV owner reaction to the electricity price based on the customer acceptance index. In: IEEE Conference on smart electrical grids technology; 2012 [In Iran].
[24] Srivastav A, Tewari A, Dong B. Baseline building energy modeling and localized uncertainty quantification using Gaussian mixture models. Energy Build 2013;65:438–47.
[25] Huilong W, Xing L, Peng X, Dengkuo Y. Short-term prediction of power consumption for large-scale public buildings based on regression algorithm. Procedia Eng 2015;121:1318–25.
[26] Ying J, Peng X, Pengfei D, Xing L. Estimating hourly cooling load in commercial buildings using a thermal network model and electricity submetering data. Appl Energy 2016;169:309–23.
[27] Li Xiwang, Wen Jin. Building energy consumption on-line forecasting using physics based system identification. Energy Build 2014;82:1–12.
[28] PJM Empirical Analysis of Demand Response Baseline Methods, 2011, PJM Load Management Task Force, Michigan.
[29] Goldberg ML, Agnew K. Development of a standard baseline calculation protocol for demand response. Seattle: Energy Program Evaluation Conference; 2003.
[30] Coughlin K, Piette MA, Goldman C, Kiliccote S. Statistical analysis of baseline load models for non-residential buildings. Energy Build 2009;41:374–81.
[31] The Demand Respond Baseline White Paper, 2011. ENERNOC, Inc, Boston.

[32] Kissock JK, Eger C. Measuring industrial energy savings. Appl Energy 2008;85:347–61.
[33] Bojuen C, Mingwei C, Chihjen L. Load forecasting using support vector machines: a study on EUNITE competition 2001. IEEE Trans Power Syst 2004;19:1821–30.
[34] Design Standard for Energy Efficiency of Public Buildings, the State Standard of the People's Republic of China; 2005.
[35] Ferrari S. Building envelope and heat capacity: re-discovering the thermal mass for winter energy savings. In: 28th AIVC Conference; 2007 [in Greece].